SUPPORTING INFORMATION

$TiNb_2O_7$ and VNb_9O_{25} of ReO_3 type in Hybrid Mg-Li Batteries: Electrochemical and Interfacial Insights

Sebastian Maletti,[a,*] Abraham Herzog-Arbeitman,[a,b] Steffen Oswald,[a] Anatoliy Senyshyn,[c] Lars Giebeler[a] and Daria Mikhailova[a,*]

[a.] *Leibniz Institute for Solid State and Materials Research (IFW) Dresden e.V., Helmholtzstraße 20, D-01069 Dresden, Germany*
[b.] *Department of Chemistry, University of Chicago, Chicago, Illinois 60637, United States*
[c.] *Forschungsneutronenquelle Heinz Maier-Leibnitz FRM-II, Technische Universität München, Lichtenbergstr. 1, D-85747 Garching bei München, Germany*

*Corresponding author

Experimental

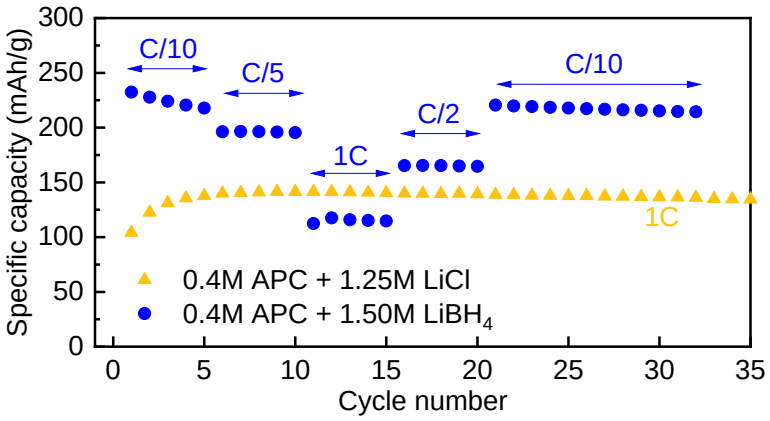

Fig. S1. Comparison of discharge capacities of $TiNb_2O_7$ in APC electrolytes using LiCl and $LiBH_4$.

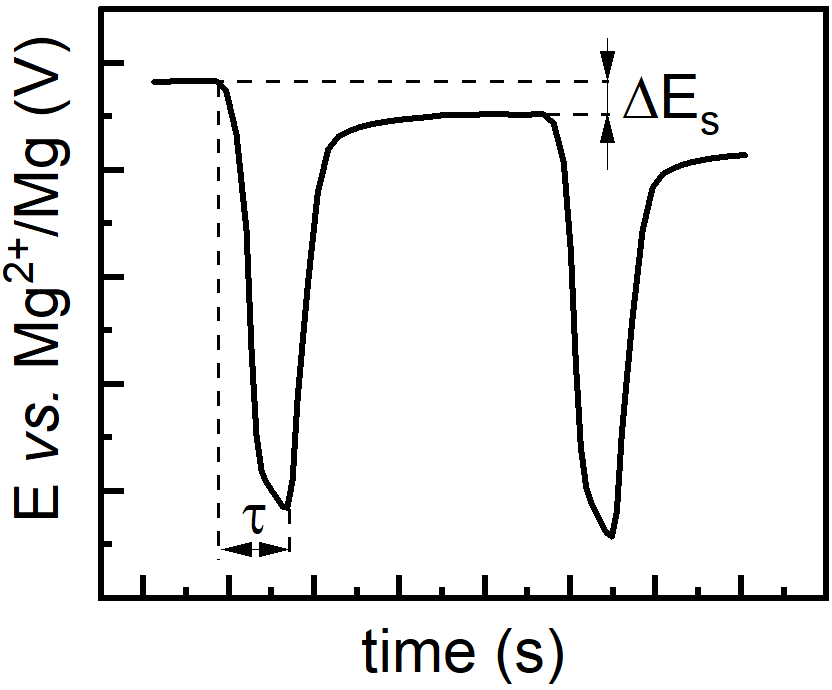

Fig. S2. Visualization of a titration step from a GITT experiment.

Structure Characterization

Table S1. Structural parameters for TNO.

Space group	*C*2/*m*	
a (Å)	20.37543(9)	
b (Å)	3.80298(1)	
c (Å)	11.89566(6)	
α (°)	90	
β (°)	120.2140(3)	
γ (°)	90	
V (Å^3)	796.543(2)	
Z	6	
Atom	Wyckoff position	(x, y, z)
(Ti,Nb)1	2*a*	(0, 0, 0)
(Ti,Nb)2	4*i*	(0.1856, 0, 0.006)
(Ti,Nb)3	4*i*	(0.0786, 0, 0.6368)
(Ti,Nb)4	4*i*	(0.8889, 0, 0.6307)
(Ti,Nb)5	4*i*	(0.2931, 0, 0.3976)
$B_{Ti,Ni}$ (Å^2)	0.500	
O1	4*i*	(0.17357, 0, 0.5970)
O2	4*i*	(0.37376, 0, 0.5815)
O3	4*i*	(0.59755, 0, 0.62250)
O4	4*i*	(0.79037, 0, 0.61590)
O5	4*i*	(0.24959, 0, 0.19460)
O6	4*i*	(0.70911, 0, 0.00140)
O7	4*i*	(0.90044, 0, 0.98630)
O8	4*i*	(0.02537, 0, 0.42000)
O9	4*i*	(0.87510, 0, 0.19000)
O10	2*b*	(0.50000, 0, 0.00000)
O11	4*i*	(0.04977, 0, 0.19790)
B_O (Å^2)	0.62(1)	
Bragg R-factor, %	4.03	
R_f-factor, %	2.69	

Table S2. Structural Parameters for VNO.

Space group	$I\bar{4}$	
a (Å)	15.69865(4)	
b (Å)	15.69865(4)	
c (Å)	3.82113(1)	
α (°)	90	
β (°)	90	
γ (°)	90	
V (Å^3)	941.709(4)	
Z	4	
Atom	Wyckoff position	(x, y, z)
V1	2*c*	(0, 0.5, 0.25)
B_V (Å^2)	0.500	
Nb1	2*a*	(0, 0, 0)
Nb2	8*g*	(0.21777, 0.10580, 0.00650)
Nb3	8*g*	(0.67333, 0.11747, -0.00130)
B_{Nb} (Å^2)	0.80(2)	
O1	8*g*	(0.48700, 0.21940, 0.49380)
O2	8*g*	(0.94860, 0.11600, -0.02830)
O3	8*g*	(0.35337, 0.15768, 0.00500)
O4	8*g*	(0.17640, 0.21628, 0.00500)
O5	8*g*	(0.25203, 0.11090, 0.50200)
O6	2*b*	(0, 0, 0.5)
O7	8*g*	(0.07504, 0.44786, 0.00100)
B_O (Å^2)	0.62(1)	
Bragg R-factor, %	3.96	
R_f-factor, %	3.88	

Electrochemical Characterization

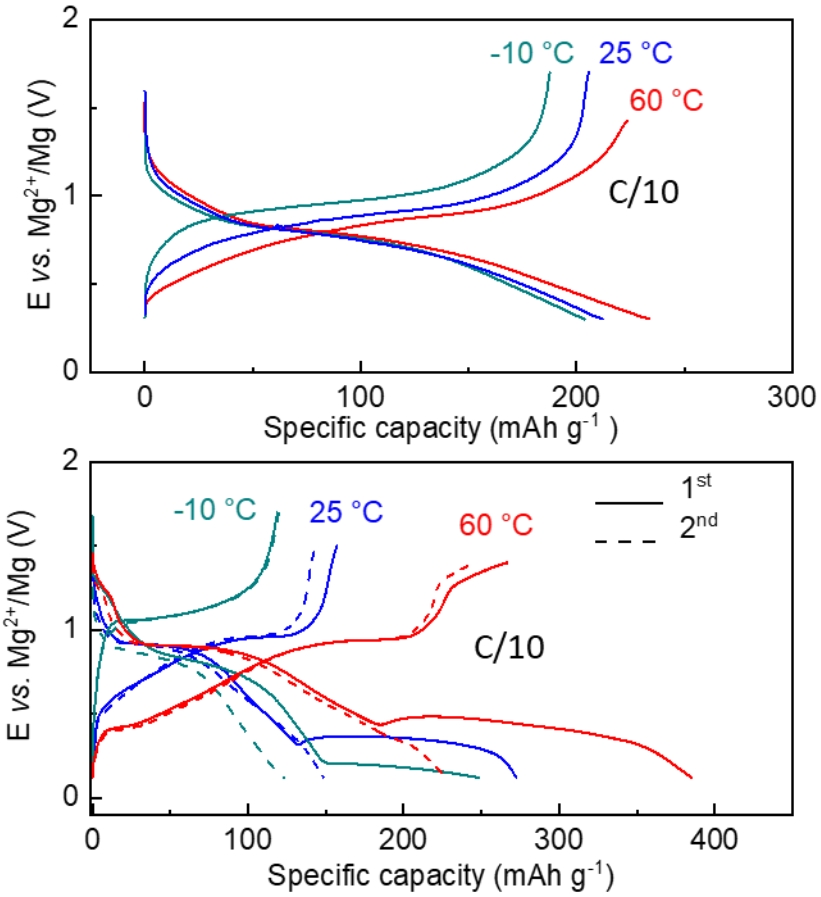

Fig. S3. First Cycles of a) TNO and b) VNO at various temperatures.

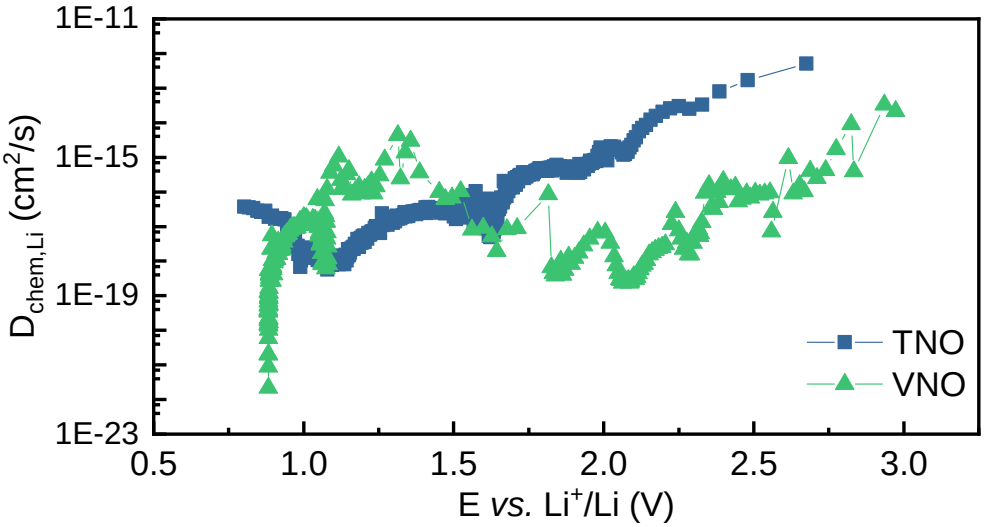

Fig. S4. Chemical Li diffusion coefficients for the lithiation process in TNO (blue) and VNO (green), calculated from GITT measurements in pure Li batteries at 25 °C.

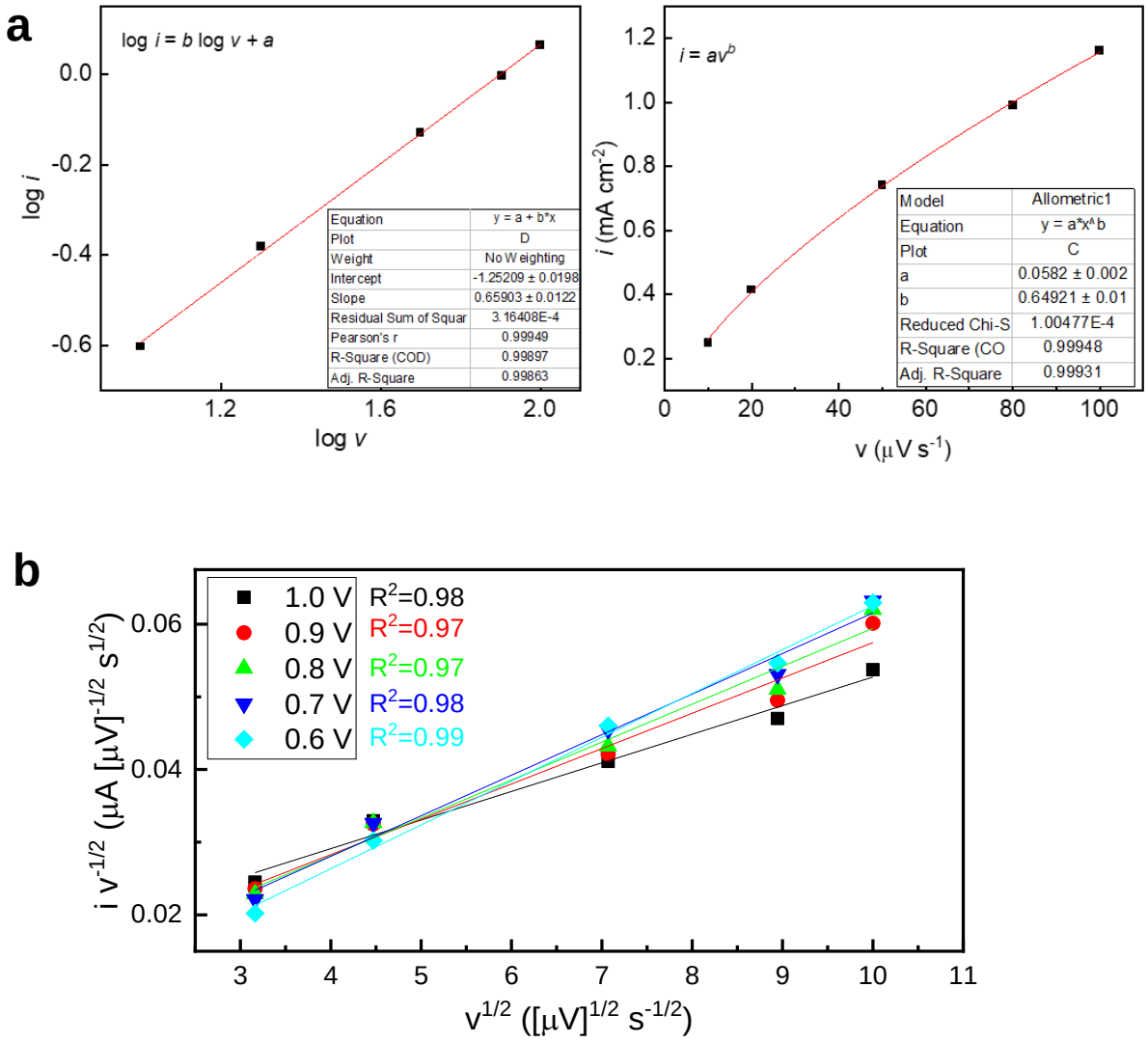

Fig. S5. a) Linear (left) and allometric (right) fit of the power-law relationship between current and sweep rate. b) Linear fits after measuring the current i at different sweep rates v. The slopes and y-axis intercepts represent capacitive and diffusion-limited contributions, respectively.

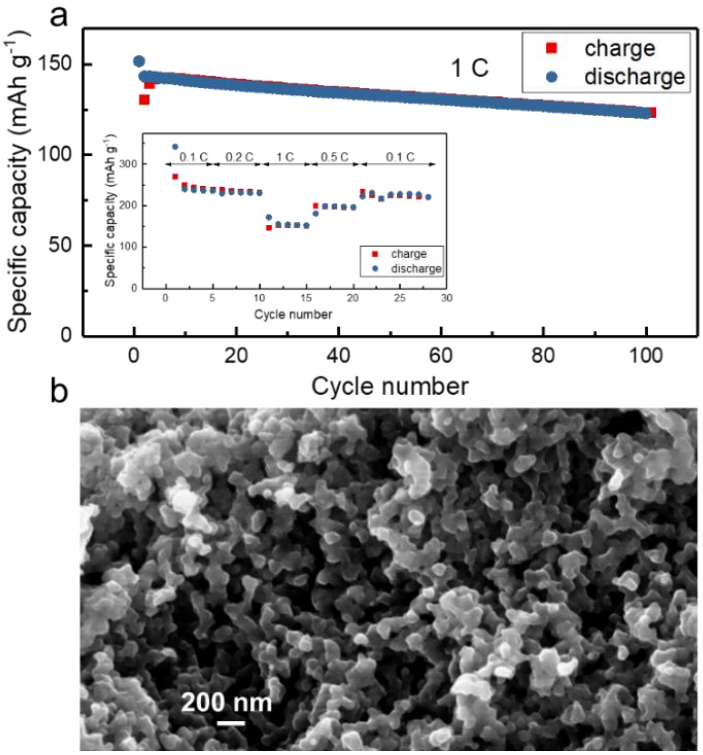

Fig. S6. a) Cycling and rate performance of TNO synthesized via the sol-gel route in hybrid Mg-Li batteries at room temperature, b) SEM micrograph of the corresponding material.

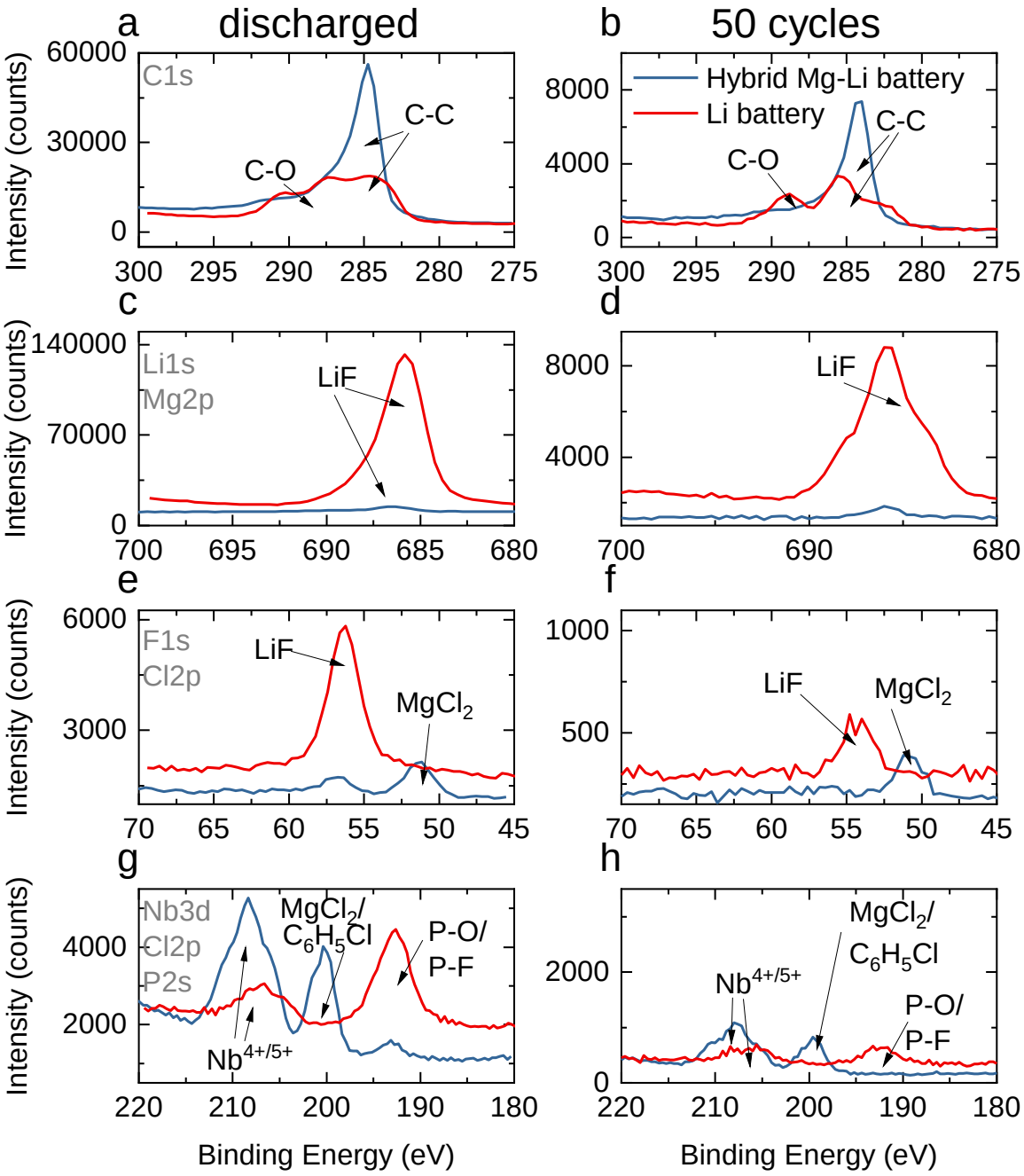

Fig. S7. X-Ray Photoelectron Spectra of the surface of a VNO electrode a,c,e,g) after the first discharge and b,d,f,h) after 50 cycles in different binding energy ranges.

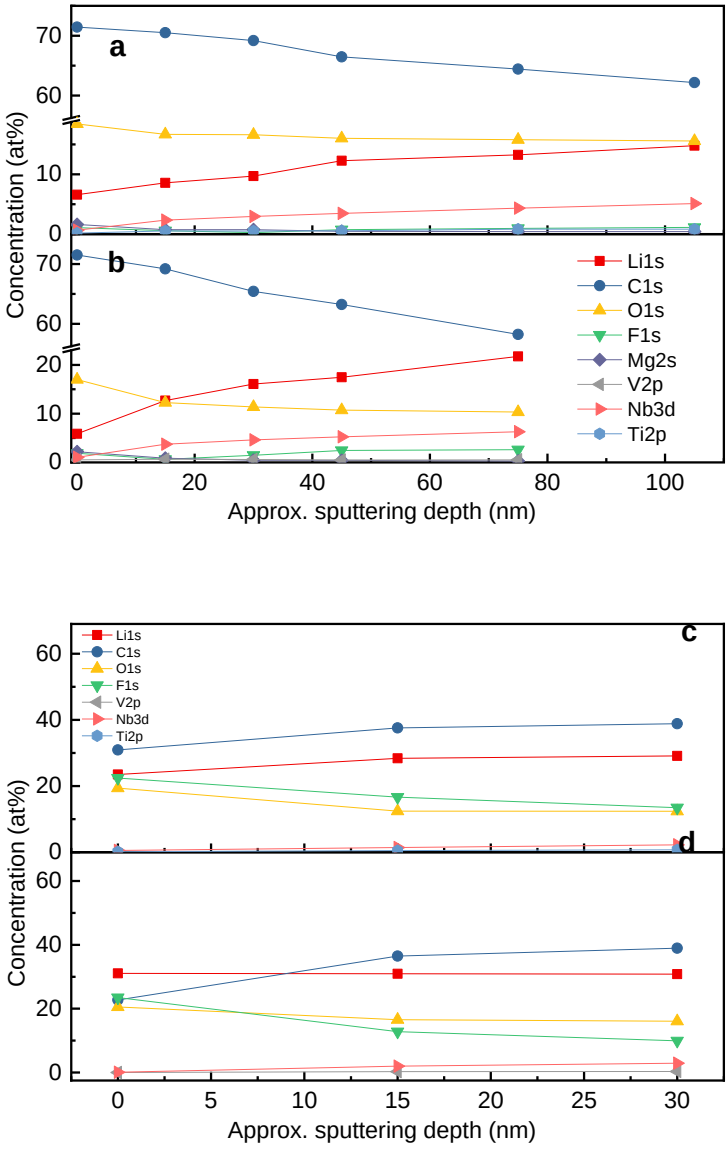

Fig. S8a. Elemental concentration depth profiles according to XPS measurements of a) TNO and b) VNO electrodes discharged in hybrid Mg-Li batteries and c) TNO, d) VNO discharged in pure Li batteries.

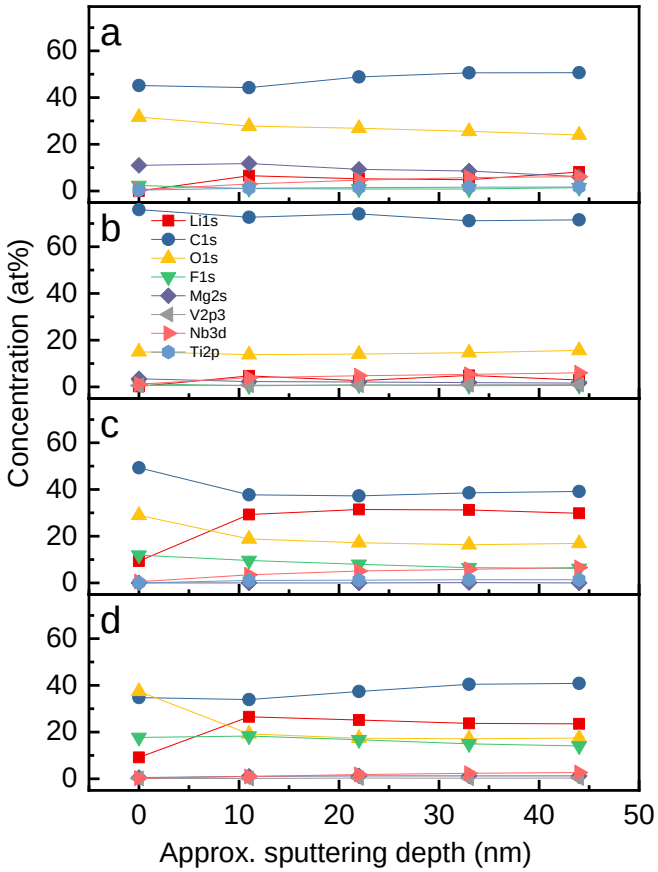

Fig. S8b. Elemental concentration depth profiles according to XPS measurements of a) TNO and b) VNO electrodes after 50 cycles in hybrid Mg-Li batteries and c) TNO, d) VNO after 50 cycles in pure Li batteries.

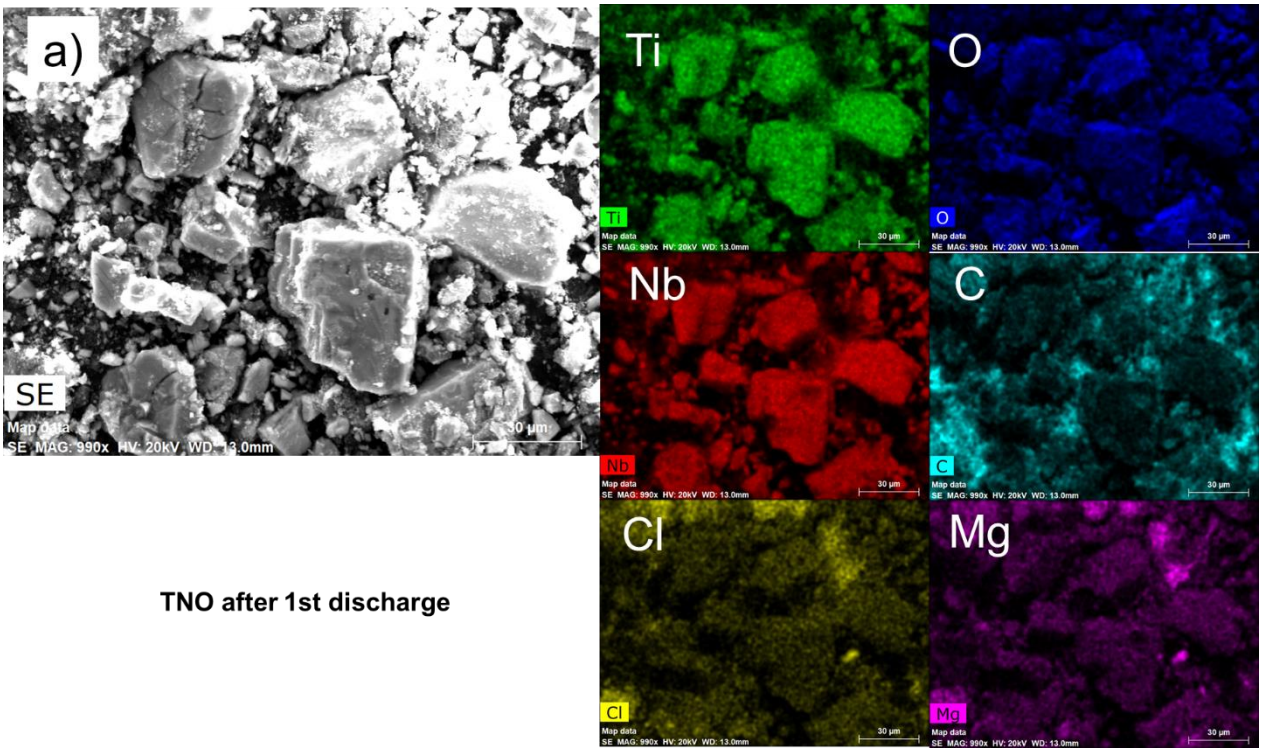

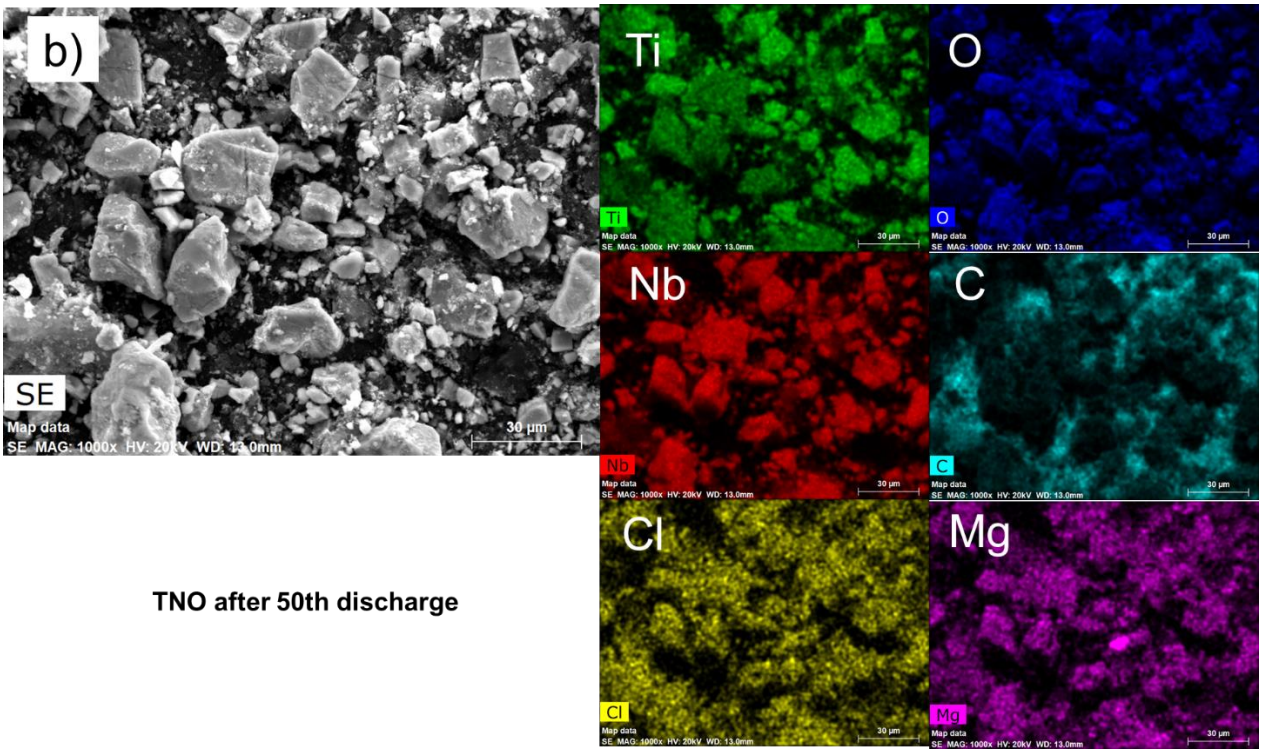

Fig. S9. EDX element mappings of a) TNO electrodes after the first discharge and b) TNO electrodes after the 50th discharge in hybrid Mg-Li batteries.